Earth, Planets and Space
a SpringerOpen Journal

LETTER

Open Access

CrossMark

Unusual low-angle normal fault earthquakes after the 2011 Tohoku-oki megathrust earthquake

Yuji Yagi[1*], Ryo Okuwaki[2], Bogdan Enescu[1] and Yukitoshi Fukahata[3]

Abstract

A few low-angle normal fault earthquakes at approximately the depth of the plate interface, with a strike nearly parallel to the trench axis, were detected immediately after the 2011 Tohoku-oki earthquake. After that, however, no such normal fault events have been observed until the occurrence of the 2014 M_W 6.6 Fukushima-oki earthquake. Here we analyze the teleseismic body waveforms of the 2014 Fukushima-oki earthquake. We first compare the observed teleseismic body waves of the 2014 Fukushima-oki earthquake with those of the largest previous low-angle normal fault aftershock (M_W 6.6), which occurred on 12 March 2011, and then estimate the centroid depth and moment tensor solution of the 2014 Fukushima-oki earthquake. The teleseismic body waves and moment tensor solution of the 2014 Fukushima-oki earthquake are similar to those of the 2011 normal fault aftershock, which suggests that the 2014 Fukushima-oki earthquake occurred at a similar depth and had a similar mechanism to that of the 2011 aftershock. We detected five low-angle normal fault aftershocks at approximately the depth of the plate interface, with a strike nearly parallel to the trench axis, and confirmed that all of them except for the 2014 Fukushima-oki earthquake occurred within 17 days after the mainshock. The occurrence of these low-angle normal fault events is likely to reflect the reversal of shear stress due to overshooting of slip during the 2011 Tohoku-oki earthquake. We speculate that a fast but heterogeneous recovery of stress state at the plate interface may explain why these events preferentially occurred immediately after the megathrust event, while one of them occurred with a significant delay. In order to better understand the characteristics of stress state in the crust, we have to carefully observe the ongoing seismic activity around this region.

Keywords: 2011 Tohoku-oki earthquake; Low-angle normal fault earthquakes; Slip overshoot

Findings

Introduction

On 11 July 2014, the Fukushima-oki, Japan, earthquake occurred in the large slip area of the 2011 Tohoku-oki earthquake (M_W 9.1). The earthquake hypocentral parameters and magnitude determined by the Japan Meteorological Agency (JMA) are as follows: origin time = 4:22 12 July 2014 (Japan Standard Time); epicenter location = (37.05° N, 142.32° E); depth = 33 km; M_{JMA} = 7.0. The fault parameters of one of the conjugate fault planes determined by the Global CMT (GCMT) project (Dziewonski et al. 1981; Ekström et al. 2012) are

dip = 27°, strike = 185°, and slip angle = −107°, with a depth of 12 km, which suggests that the 2014 Fukushima-oki earthquake was a low-dip-angle normal fault event, at approximately the depth of the plate interface, with a strike nearly parallel to the trench axis (http://www.globalcmt.org; last access on 13 February 2015).

After the 2011 Tohoku-oki earthquake, a few low-angle normal fault earthquakes were detected at approximately the depth of the plate interface. These events have been interpreted as being due to slip overshoot during the 2011 Tohoku-oki earthquake (Ide et al. 2011; Yagi and Fukahata 2011), in relation to the drastic change of focal mechanisms around the large slip area (Asano et al. 2011) and nearly complete stress drop along the plate interface (Hasegawa et al. 2011; Yagi and

* Correspondence: yagi-y@geol.tsukuba.ac.jp
[1]Faculty of Life and Environmental Sciences, University of Tsukuba, Tennodai 1-1-1, Tsukuba 305-8572, Japan
Full list of author information is available at the end of the article

Springer

Yagi *et al. Earth, Planets and Space* (2015) 67:100

Page 2 of 7

Fukahata 2011). Figure 1 shows the distribution of stress drop of the 2011 Tohoku-oki earthquake calculated from the distribution of moment release (Fukahata et al. 2012) together with the focal mechanism of the largest

low-angle normal fault event (M_W 6.6) that occurred just after the 2011 Tohoku-oki earthquake (Yagi and Fukahata 2011) as well as that of the 2014 Fukushima-oki earthquake. As shown in Fig. 1, these earthquakes occurred in
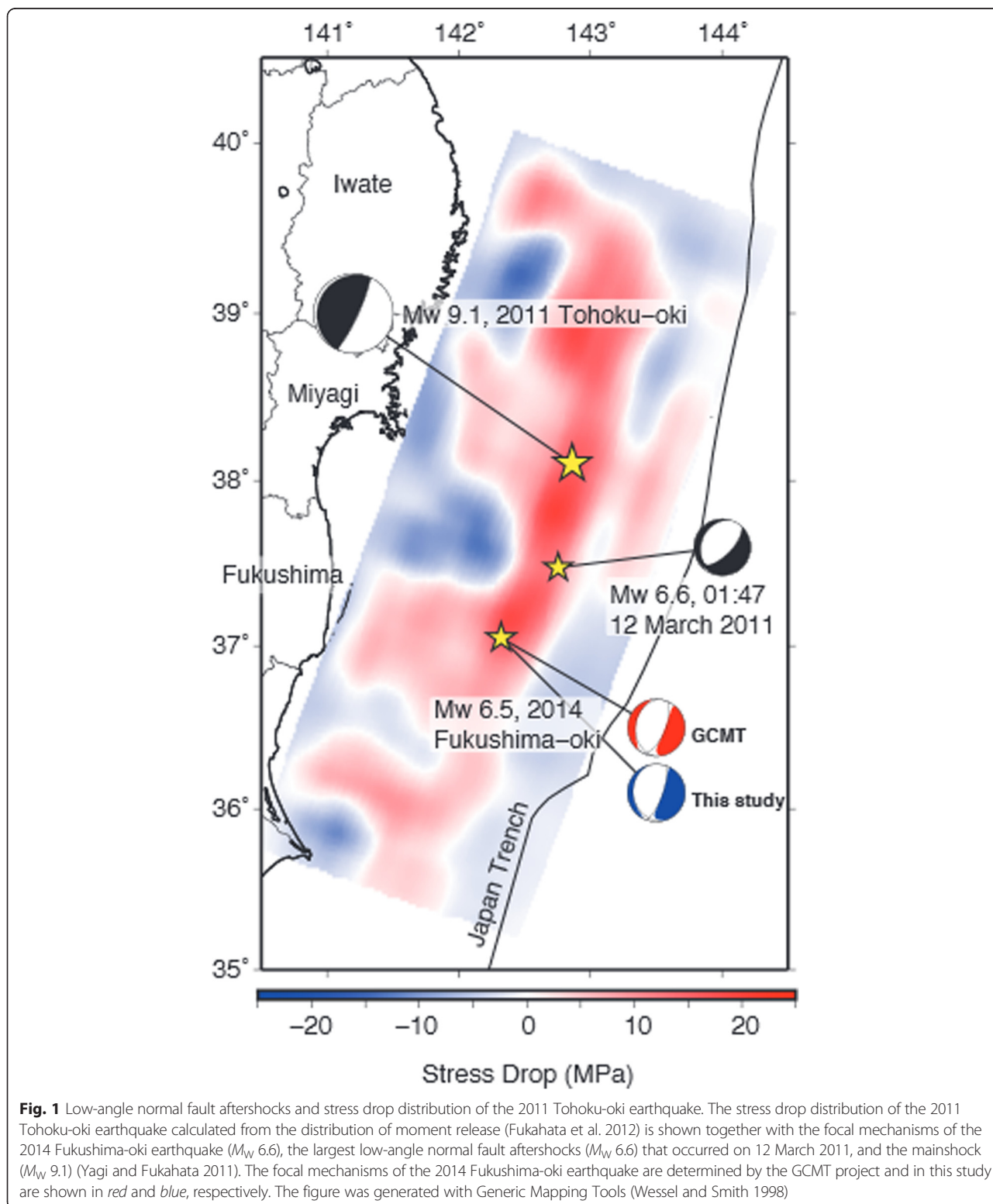

Fig. 1 Low-angle normal fault aftershocks and stress drop distribution of the 2011 Tohoku-oki earthquake. The stress drop distribution of the 2011 Tohoku-oki earthquake calculated from the distribution of moment release (Fukahata et al. 2012) is shown together with the focal mechanisms of the 2014 Fukushima-oki earthquake (M_W 6.6), the largest low-angle normal fault aftershocks (M_W 6.6) that occurred on 12 March 2011, and the mainshock (M_W 9.1) (Yagi and Fukahata 2011). The focal mechanisms of the 2014 Fukushima-oki earthquake are determined by the GCMT project and in this study are shown in *red* and *blue*, respectively. The figure was generated with Generic Mapping Tools (Wessel and Smith 1998)

Yagi *et al. Earth, Planets and Space* (2015) 67:100

Page 3 of 7

the area of large stress drop of the 2011 Tohoku-oki earthquake.

In general, the teleseismic body waves contain information on the depth range of the rupture area, since the shape of the theoretical waveforms varies with depth, as a consequence of the different timing of the reflected phases (e.g., pP and sP). In this study, we compare the observed teleseismic body waves of the 2014 Fukushima-oki earthquake with those of the largest low-angle normal fault aftershock and then estimate the centroid depth and moment tensor solution of the 2014 Fukushima-oki earthquake. We also extract low-angle normal fault earthquake activity at approximately the depth of the plate interface and discuss the occurrence mechanism of the 2014 Fukushima-oki earthquake.

Teleseismic body waveforms

We collected teleseismic P-wave data recorded at 33 broadband network stations (Fig. 2a) for the 2014 Fukushima-oki earthquake, as well as for the largest low-angle normal fault event that occurred at 1:47 on 12 March 2011 (UTC). In Fig. 2b, we compare the observed

waveforms of the two earthquakes at each recording station; we have applied a Butterworth band-pass filter between 0.005 and 0.04 Hz in order to mitigate the effect of rupture process complexity and low-frequency noise. In general, the shape of theoretical waveforms depends on the hypocenter depth and focal mechanism. As shown in Fig. 2b, the teleseismic body waves of the 2014 Fukushima-oki earthquake are similar to those of the 12 March 2011 low-angle normal fault event. The close resemblance of the teleseismic body waves strongly suggests that the 2014 Fukushima-oki earthquake occurred at a similar depth and had a similar mechanism to that the 2011 aftershock. As analyzed by Yagi and Fukahata (2011) (see Figure S4 of their paper), the 12 March 2011 event occurred at approximately the depth of the plate interface with a strike nearly parallel to the trench axis. Hence, the 2014 Fukushima-oki earthquake can be reasonably considered to have occurred at approximately the depth of the plate interface with a strike nearly parallel to the trench axis. Figure 3 shows the observed waveforms as a function of station azimuth. The waveform pulses are relatively broad at westward. This observation suggests that the rupture propagated mainly eastward.
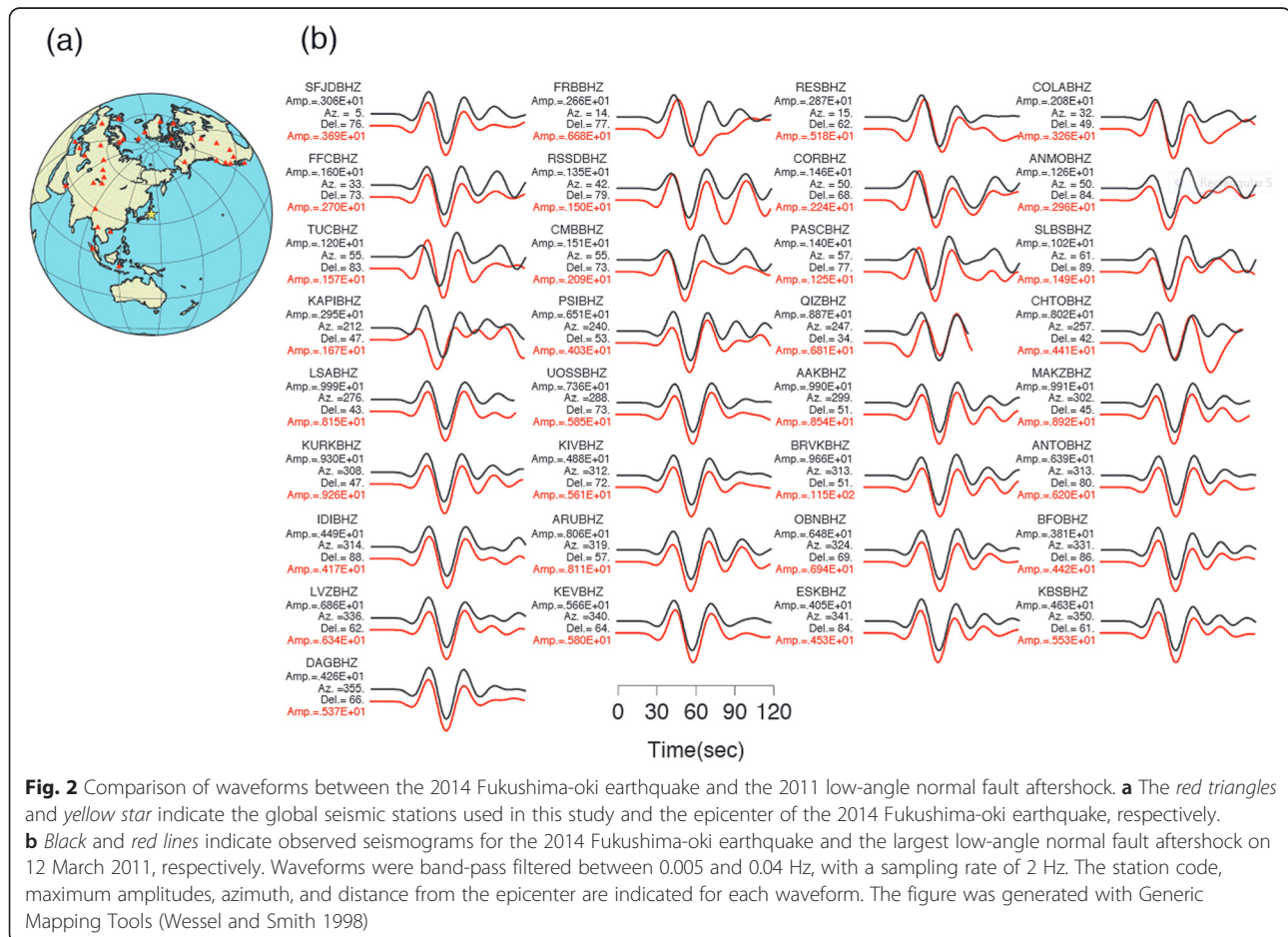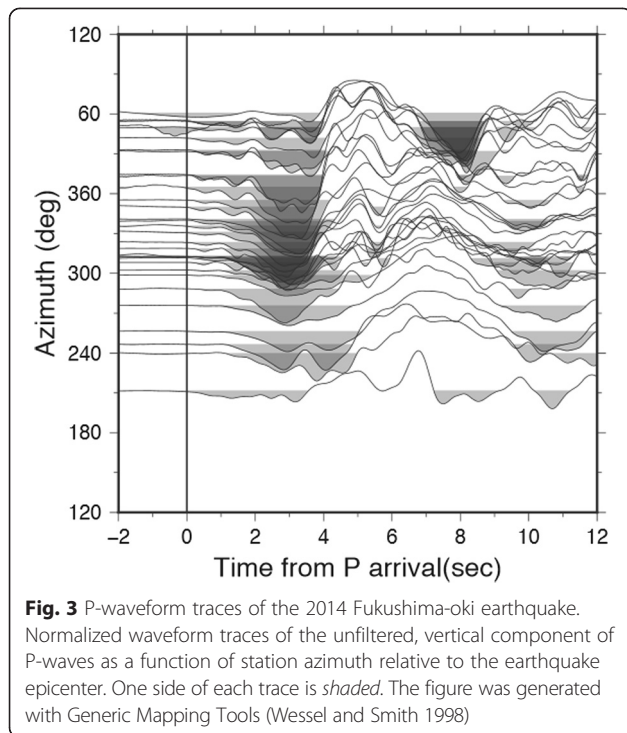

Fig. 2 Comparison of waveforms between the 2014 Fukushima-oki earthquake and the 2011 low-angle normal fault aftershock. **a** The *red triangles* and *yellow star* indicate the global seismic stations used in this study and the epicenter of the 2014 Fukushima-oki earthquake, respectively. **b** *Black* and *red lines* indicate observed seismograms for the 2014 Fukushima-oki earthquake and the largest low-angle normal fault aftershock on 12 March 2011, respectively. Waveforms were band-pass filtered between 0.005 and 0.04 Hz, with a sampling rate of 2 Hz. The station code, maximum amplitudes, azimuth, and distance from the epicenter are indicated for each waveform. The figure was generated with Generic Mapping Tools (Wessel and Smith 1998)

Yagi *et al. Earth, Planets and Space* (2015) 67:100

Page 4 of 7

Fig. 3 P-waveform traces of the 2014 Fukushima-oki earthquake. Normalized waveform traces of the unfiltered, vertical component of P-waves as a function of station azimuth relative to the earthquake epicenter. One side of each trace is *shaded*. The figure was generated with Generic Mapping Tools (Wessel and Smith 1998)

Moment tensor solution

We applied the moment tensor inversion to the collected teleseismic body waveforms of the 2014 Fukushima-oki earthquake. The observed waveforms were shifted on the basis of their first arrival time and then converted into displacement waveforms with a sampling rate of 2 Hz; after that, a Butterworth band-pass filter between 0.005 and 0.04 Hz was applied. The theoretical Green's function was calculated by the method of Kikuchi and Kanamori
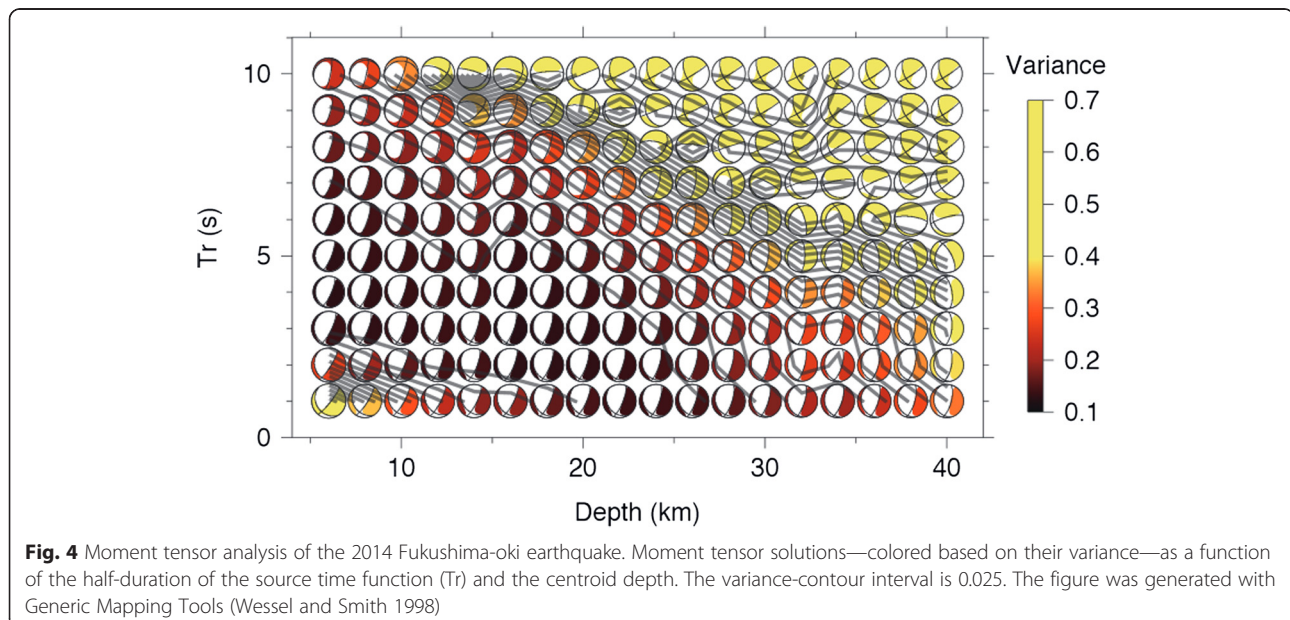
(1991) for the preliminary reference Earth model (PREM; Dziewonski and Anderson 1981). In Fig. 4, we show the distribution of waveform variance as a function of the half-duration of the source time function (Tr) and the centroid depth.

As can be seen in Fig. 4, the smallest variance area corresponds to a centroid depth from 6 to 30 km. The focal mechanism solution of the small variance area shows that one of the two possible fault motions is characterized by low-angle normal faulting. As shown in Fig. 3, the rupture propagated mainly eastward from the hypocenter, and the high-angle fault plane is inconsistent with the characteristic of the observed waveforms. The strike and dip of the low-angle normal faulting are about 170° and 21°, respectively, which is consistent with the geometry of the plate interface. These results show that observed waveforms can be well explained by back slip motion along the plate interface. A result of finite fault inversion also supports this interpretation (Additional file 1: Figure S1). The total seismic moment (M_0) is 9.6×10^{18} Nm ($M_W = 6.6$), which is in agreement with the GCMT solution: 7.8×10^{18} Nm (http://www.globalcmt.org; last access on 13 February 2015).

Seismicity of low-angle normal fault earthquakes

We investigated the aftershock activity of the 2011 Tohoku-oki earthquake by focusing on the low-angle normal fault earthquakes that are likely to have occurred at the plate interface.

We searched for low-angle normal fault earthquakes through the GCMT Catalog from 11 March 2011 to 31 December 2014, by using the following criteria: $150° \leq$ strike $\leq 240°$, dip $\leq 30°$, $-135° \leq$ rake $\leq -45°$, and depth $\leq$

Fig. 4 Moment tensor analysis of the 2014 Fukushima-oki earthquake. Moment tensor solutions—colored based on their variance—as a function of the half-duration of the source time function (Tr) and the centroid depth. The variance-contour interval is 0.025. The figure was generated with Generic Mapping Tools (Wessel and Smith 1998)

Yagi *et al. Earth, Planets and Space* (2015) 67:100

Page 5 of 7

60 km, in the area shown in Fig. 5a. A total of eight normal fault earthquakes correspond to these criteria (Fig. 5a), and they are plotted on the magnitude-time diagram (Fig. 5b). However, some of the earthquakes that satisfy the above criteria are quite far from the depth of the plate interface, which is shown by contour lines in Fig. 5a (Nakajima and Hasegawa 2006; Hirose et al. 2008; Nakajima et al. 2009; Kita et al. 2010). Because of the depth discrepancy, these earthquakes (blank stars in Fig. 5a) cannot be considered to have occurred at the plate interface. After eliminating these earthquakes, we found that four of the five interplate normal fault earthquakes are likely to have occurred just after the Tohoku-oki earthquake (i.e., within 17 days from 11 March 2011). The 2014 Fukushima-oki earthquake is the first low-angle normal fault event at approximately the depth of the plate interface since the end of March 2011.

Discussion

Previous studies (e.g., Asano et al. 2011) analyzed seismicity immediately after the 2011 Tohoku-oki earthquake and reported the occurrence of many normal fault aftershocks. Most of them occurred near the trench and in the outer-rise of the Pacific plate, while some occurred along the coastal area of Japan. Just a few low-angle normal fault events were detected, and they have been interpreted as interplate aftershocks that indicate the reversal of shear stress due to overshooting of slip during the 2011 Tohoku-oki earthquake (Ide et al. 2011; Yagi and Fukahata 2011). However, it should be emphasized that low-angle normal fault earthquakes at approximately the depth of the plate interface are unusual in subduction zones.

Yagi and Fukahata (2011) have demonstrated that the largest low-angle normal fault event on 12 March 2011 (Fig. 1) occurred at approximately the depth of the plate interface with a strike nearly parallel to the trench axis. Based on the inversion analysis of waveform data, they have also confirmed that the fault slip certainly occurred along the low-angle fault plane not along the conjugate high-angle plane based on the inversion analysis of waveform data. The close resemblance of the observed waveforms between the 2014 Fukushima-oki and the 12 March 2011 earthquakes strongly suggests that the 2014 Fukushima-oki earthquake is also a low-angle normal fault event at approximately the depth of the plate interface with a strike nearly parallel to the trench axis. The
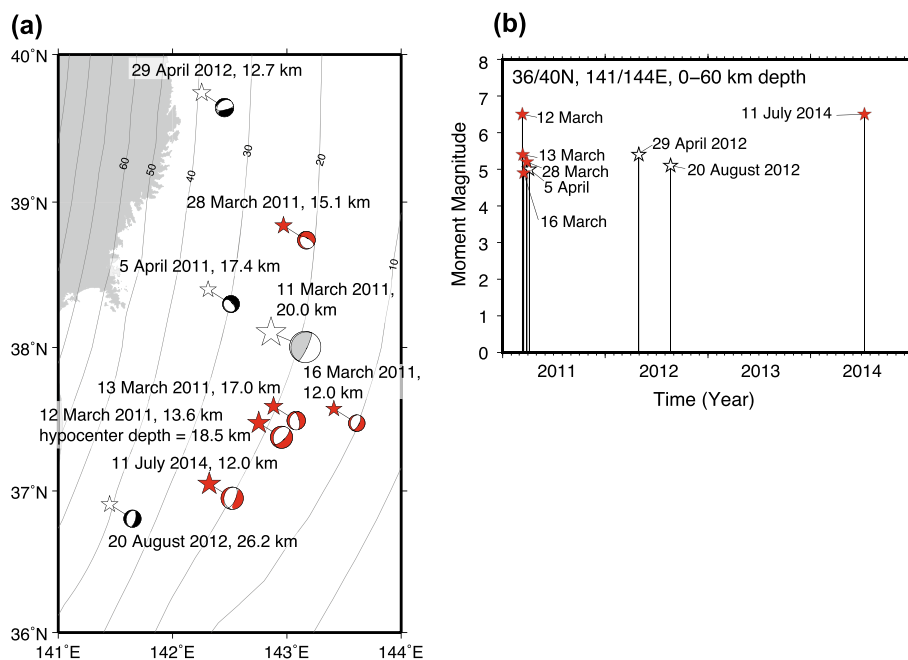

Fig. 5 Spatial distribution and magnitude-time plot of low-angle normal fault earthquakes. **a** *Stars* denote the epicenters of earthquakes, whose locations are derived from the JMA unified hypocenter catalog. *Red stars* indicate the low-angle normal fault earthquakes resembling the 2014 Fukushima-oki earthquake, and *small blank stars* represent the other normal fault earthquakes. Focal mechanisms were determined by the GCMT project. The size of stars and focal mechanisms are proportional to the magnitude. The centroid depth of the GCMT solution together with the earthquake occurrence date is specified for Earth event. The hypocenter depth of the 2011 low-angle normal fault aftershock determined by Yagi and Fukahata (2011) is also shown. In general, the GCMT solution has poor depth resolution. The iso-depth contours of the subducting plate interface are drawn every 10 km. **b** *Red stars* indicate the low-angle normal fault earthquakes resembling the 2014 Fukushima-oki earthquake, and *blank stars* represent the other normal fault earthquakes. The moment magnitude of each event was determined by the GCMT project. The figure was generated with Generic Mapping Tools (Wessel and Smith 1998)

Yagi *et al. Earth, Planets and Space* (2015) 67:100

Page 6 of 7

moment tensor inversion (Fig. 4) supports this idea, although the centroid depth of the 2014 Fukushima-oki earthquake cannot be as sharply determined as for the 2012 event because the 2014 event has a shorter duration of the source time function. Both events occurred in the large stress drop area of the 2011 Tohoku-oki earthquake, which is also consistent with the idea that the slip overshoot during the 2011 Tohoku-oki earthquake has triggered the 2014 Fukushima-oki earthquake as well as the 12 March 2011 earthquake.

Some studies (e.g., Ide et al. 2011; Hasegawa et al. 2011; Yagi and Fukahata 2011) have advocated that the fault rupture during the 2011 Tohoku-oki earthquake released most of the tectonically accumulated stress. This has recently been shown to correspond with an immediate increase of the *b*-value parameter (i.e., the slope of the frequency-magnitude distribution of earthquakes) after the 2011 Tohoku-oki earthquake, along the mainshock rupture region (Tormann et al. 2015). However, the large post-seismic slip in the down-dip region (e.g., Ozawa et al. 2011) and viscoelastic relaxation in the asthenosphere (Watanabe et al. 2014; Yamagiwa et al. 2015) have contributed to the recovery of stress in the large slip area of the 2011 Tohoku-oki earthquake. A fast recovery has been inferred recently from the return of *b*-values to pre-mainshock levels by September 2014 (Tormann et al. 2015). Stress inversion analysis using focal mechanism data (Hardebeck 2012) seems to point out a similar fast recovery to pre-Tohoku stress levels. The rapid recovery of stress state should restrain the activity of low-angle normal fault earthquakes at approximately the depth of the plate interface. In fact, we have not found similar events since the end of March 2011 until 11 July 2014 (Fig. 5b). Nevertheless, the 2014 Fukushima-oki earthquake has happened. What does the occurrence of this earthquake mean from a geophysical point of view?

We hypothesize that such occurrences are related to the strong spatial heterogeneity of stress state in the crust. In the case of the 2011 Tohoku-oki earthquake, it is almost impossible to detect spatial heterogeneity of slip with a length scale of a few tens of kilometers from inversion analyses of geodetic and seismic data. Hence, due to several possible reasons (e.g., strong patches, dynamic effects), strong spatial heterogeneity of stress could have been produced by the 2011 Tohoku-oki earthquake. In addition, the stress recovery process can contribute to enhance the spatial heterogeneity of stress; indeed, the result of Tormann et al. (2015) implies that there are small patches along the megathrust where the stress recovery could be significantly delayed. Such patches may initiate rare normal-fault events like the 2014 Fukushima-oki earthquake. The decrease of fault strength due to an increase of pore fluid pressure might have further encouraged the occurrence of such "anomalous" events. Note that fluids are abundant at or close to the plate interface (e.g., Matsubara and Obara 2011). In order to better understand the characteristics of stress state, in particular the evolution of spatial heterogeneity in a short and long term, we have to carefully observe the ongoing seismic activity around this region.

Additional file

Additional file 1: Figure S1. The finite fault inversion analysis of the 2014 Fukushima-oki earthquake. (a) Estimated total slip distribution (map view). We inverted teleseismic P-wave data recorded at 26 broadband network stations, which were selected to ensure adequate azimuthal coverage and data quality. We assumed that the faulting occurred on a single plane and adopted an epicenter (37.05° N, 142.32° E) and fault mechanism (strike 170°, dip 21°) that were inferred from the JMA seismicity and the result of the moment tensor inversion analysis. The same depth of the hypocenter as for 12 March 2011 low-angle normal fault aftershock determined by Yagi and Fukahata (2011) was assumed in this analysis. Star indicates the epicenter of the 2014 Fukushima-oki earthquake. Also shown are the focal mechanism determined in this analysis and the 1-day aftershocks (black dots), determined by the JMA. (b) The moment-rate function. (c) Black and red lines indicate observed and synthetic velocity seismograms band-pass filtered between 0.005 and 4.5 Hz with a sampling rate of 10 Hz, respectively. The good fit of the synthetic seismograms by the observed ones shows that the 2014 Fukushima-oki earthquake occurred at a similar depth and had a similar mechanism with that of the 12 March 2011 aftershock. The figures were generated with Generic Mapping Tools (Wessel and Smith 1998).

Author details
[1]Faculty of Life and Environmental Sciences, University of Tsukuba, Tennodai 1-1-1, Tsukuba 305-8572, Japan. [2]Graduate School of Life and Environmental Sciences, University of Tsukuba, Tennodai 1-1-1, Tsukuba 305-8572, Japan. [3]Disaster Prevention Research Institute, Kyoto University, Uji, Kyoto 611-0011, Japan.

References
Asano Y, Saito T, Ito Y, Shiomi K, Hirose H (2011) Spatial distribution and focal mechanisms of aftershocks of the 2011 off the Pacific coast of Tohoku Earthquake. Earth Planets Space 63:669–673. doi:10.5047/eps.2011.06.016

Yagi *et al. Earth, Planets and Space* (2015) 67:100

Page 7 of 7

Dziewonski AM, Anderson DL (1981) Preliminary reference Earth model. Phys Earth Planet Inter 25:297–356. doi:10.1016/0031-9201(81)90046-7

Dziewonski AM, Chou TA, Woodhouse JH (1981) Determination of earthquake source parameters from waveform data for studies of global and regional seismicity. J Geophys Res 86:2825–2852. doi:10.1029/JB086iB04p02825

Ekström G, Nettles M, Dziewoński AM (2012) The global CMT project 2004–2010: centroid-moment tensors for 13,017 earthquakes. Phys Earth Planet Inter 200–201:1–9. doi:10.1016/j.pepi.2012.04.002

Fukahata Y, Yagi Y, Mitsui Y (2012) Absolute strain release in the 2011 Tohoku-oki Earthquake. J Geol Soc Japan 118:396–409. doi:10.5575/geosoc.2012.0040 (in Japanese with English abstract)

Hardebeck JL (2012) Coseismic and postseismic stress rotations due to great subduction zone earthquakes. Geophys Res Lett 39:L21313. doi:10.1029/2012GL053438

Hasegawa A, Yoshida K, Okada T (2011) Nearly complete stress drop in the 2011 M_W 9.0 off the Pacific coast of Tohoku Earthquake. Earth Planets Space 63:703–707. doi:10.5047/eps.2011.06.007

Hirose F, Nakajima J, Hasegawa A (2008) Three-dimensional seismic velocity structure and configuration of the Philippine Sea slab in southwestern Japan estimated by double-difference tomography. J Seismol Soc Japan 113:123–138. doi:10.1029/2007JB005274 (in Japanese with English abstract)

Ide S, Baltay A, Beroza GC (2011) Shallow dynamic overshoot and energetic deep rupture in the 2011 Mw 9.0 Tohoku-Oki earthquake. Science 332:1426–1429. doi:10.1126/science.1207020

Kikuchi M, Kanamori H (1991) Inversion of complex body waves—III. Bull Seismol Soc Am 81:2335–2350

Kita S, Okada T, Hasegawa A, Nakajima J, Matsuzawa T (2010) Anomalous deepening of a seismic belt in the upper-plane of the double seismic zone in the Pacific slab beneath the Hokkaido corner: possible evidence for thermal shielding caused by subducted forearc crust materials. Earth Planet Sci Lett 290:415–426. doi:10.1016/j.epsl.2009.12.038

Matsubara M, Obara K (2011) The 2011 off the Pacific coast of Tohoku Earthquake related to a strong velocity gradient with the Pacific plate. Earth Planets Space 63:663–667. doi:10.5047/eps.2011.05.018

Nakajima J, Hasegawa A (2006) Anomalous low-velocity zone and linear alignment of seismicity along it in the subducted Pacific slab beneath Kanto, Japan: reactivation of subducted fracture zone? Geophys Res Lett 33:L36309. doi:10.1029/2006GL026773

Nakajima J, Hirose F, Hasegawa A (2009) Seismotectonics beneath the Tokyo metropolitan area, Japan: effect of slab-slab contact and overlap on seismicity. J Geophys Res 114:B08309. doi:10.1029/2008JB006101

Ozawa S, Nishimura T, Suito H, Kobayashi T, Tobita M, Imakiire T (2011) Coseismic and postseismic slip of the 2011 magnitude-9 Tohoku-Oki earthquake. Nature 475:373–377. doi:10.1038/nature10227

Tormann T, Enescu B, Woessner J, Wiemer S (2015) Randomness of megathrust earthquakes implied by rapid stress recovery after the Japan earthquake. Nat Geosci 8:152–158. doi:10.1038/ngeo2343

Watanabe S, Sato M, Fujita M, Ishikawa T, Yokota Y, Ujihara N, Asada A (2014) Evidence of viscoelastic deformation following the 2011 Tohoku-Oki earthquake revealed from seafloor geodetic observation. Geophys Res Lett 41:5789–5796. doi:10.1002/2014GL061134

Wessel P, Smith WHF (1998) New, improved version of generic mapping tools released. Eos, Trans Am Geophys Union 79:579–579. doi:10.1029/98EO00426

Yagi Y, Fukahata Y (2011) Rupture process of the 2011 Tohoku-oki earthquake and absolute elastic strain release. Geophys Res Lett 38:1–6. doi:10.1029/2011GL048701

Yamagiwa S, Miyazaki S, Hirahara K, Fukahata Y (2015) Afterslip and viscoelastic relaxation following the 2011 Tohoku-oki earthquake (Mw9.0) inferred from inland GPS and seafloor GPS/acoustic data. Geophys Res Lett 42:66–73. doi:10.1002/2014gl061735